ELSEVIER

Carbohydrate Research 263 (1994) 13–24

CARBOHYDRATE
RESEARCH

# A quantitative approach to describe the overall motion of monosaccharides in solution. A $^{13}$C NMR relaxation study of 1,6-anhydro-β-D-glucopyranose in dimethyl sulfoxide

Photis Dais

*Department of Chemistry, University of Crete, 71409 Iraklion, Crete, Greece*

Received 10 November 1993; accepted in revised form 27 April 1994

---

## Abstract

Quantitative aspects describing the dynamics of monosaccharides in solution by employing $^{13}$C NMR relaxation are reported in this work. This method has been applied to analyze the variable temperature $^{13}$C spin-lattice relaxation times of 1,6-anhydro-β-D-glucopyranose, which appears to tumble anisotropically in dimethyl sulfoxide solution.

*Keywords:* $^{13}$C NMR; 1,6-Anhydro-β-D-glucopyranose in $Me_2SO$

---

## 1. Introduction

$^{13}$C Nuclear magnetic relaxation has long been employed to monitor molecular motion in solution, and has been extensively used to study the dynamics of small and large molecules [1]. A large number of relaxation experiments [2–4] have been carried out recently to probe variations in overall and internal mobility of monosaccharides. However, the majority of these studies interpret the relaxation data in a qualitative manner, and only a few reports [5–8] attempt to analyze the dynamics of monosaccharides by employing explicit time-correlation functions (TCF) (dynamic models).

Although qualitative analysis of the $^{13}$C relaxation data appears to be useful for describing the gross features of mobility, it is likely to be less valuable than quantitative information inherent in the measured $^{13}$C relaxation parameters. Worse than that, superficial interpretation of the relaxation data may lead to totally erroneous conclusions about the true dynamic properties of a monosaccharide in solution. For instance, the overall motion of the majority of hexopyranoses and derivatives has been described [9–11] as isotropic despite the fact that sizeable differences, well outside the experimental error, have been observed in the

*SSDI* 0008-6215(94)00159-D

spin-lattice relaxation times ($T_1$) of the endocyclic ring carbons. In other instances, anisotropic motion has been identified [10] on the basis of the shorter $T_1$ value of a $^{13}C$ ring nucleus as compared to those of the remaining ring carbon nuclei, indicating the presence of a preferred axis of rotation, the general direction of which is assumed to be parallel, or nearly so, to the relevant $^{13}C-^{1}H$ vector. Such a simple treatment, however, may lead to misinterpretation of the observed data [7,12].

The major objectives of this paper are to introduce some fundamental quantitative considerations in modelling the dynamics of the overall motion of monosaccharides in solution, and to apply this knowledge to describing the overall motion of 1,6-anhydro-β-D-glucopyranose (**1**) in dimethyl sulfoxide solution. This rigid molecule contains a number of non-equivalent $^{13}C-^{1}H$ vectors and is amenable to a rigorous quantitative treatment.

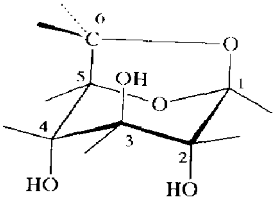

## 2. Experimental

*$^{13}C$ NMR relaxation measurements.*—$^{13}C$ Spin-lattice relaxation time measurements were conducted, under noise modulated proton decoupling conditions, on a Bruker AC200F spectrometer operating at 50.3 MHz for the $^{13}C$ nucleus by using the IRFT method. Typically 8–10 samples of the recovery magnetizations were taken. These were then subjected to three parameters non-linear least squares analysis to yield $T_1$ data. Repeated measurements of the relaxation times at a given temperature were reproducible to within $\pm 2\%$. The overall accuracy of the $T_1$ data collected in Table 1 is estimated to be $\pm 5\%$ or better. $^{13}C$ NOEs were measured by the inverse gated decoupling technique. The waiting time between 90° pulses was maintained for longer than $10 \times T_1$. 50 transients were accumulated in each run to obtain reproducible and accurate determinations. Relative intensities were taken as peak heights after the application of an exponential line broadening of about three times the normal linewidths.

Sample temperatures were monitored before and after each measurement by using a precalibrated thermocouple in the probe insert. The temperatures were accurate to within $\pm 1°C$.

Compound **1** was obtained from Aldrich and used without further purification. Solutions of 0.5 M in deuterated dimethyl sulfoxide were degassed by the usual freeze–pump–thaw technique and sealed in 5-mm NMR tubes before use.

*Numerical Calculations.*—The first routine ATCOR2 [13a] was used to calculate the coordinates of atoms, the moment of inertia tensor, the directional cosines of the principal axes, and the principal moments of inertia, $I_{xx}$, $I_{yy}$, and $I_{zz}$. The same results were obtained using the pertinent subroutines involved in the MOLDYN program [13b]. The molecular geometry of **1** could be obtained from its crystal structure [14]. $^1$H NMR studies [15] have shown that the rigid structure of **1** in the solid form is retained in solution. It was found [14,15] that the pyranose ring of the molecule has the $^1C_4$ chair conformation, which is distorted by the formation of the anhydride. The three hydroxyl substituents are axial relative to the pyranosyl ring, two *exo*-axial at C-2 and C-4, and one *endo*-axial at C-3.

The crystal structure determined by X-ray diffraction provides coordinates for the carbon atoms of **1**, but as usual the hydrogen atoms could not be located with sufficient precision. Thus, the C-H bond lengths tend to be shorter than the mean internuclear separation. On the other hand, adopting the same conventional values (1.09, 1.10, or 1.11 Å) for all the C–H bond lengths in the molecule is an insufficient method that may obscure any differences in the observed $T_1$ values of the corresponding carbon atoms arising from differences in molecular motion.

A common approach to obtain C–H bond lengths, provided that there are no other experimental sources, is the use of quantum mechanical calculations. This procedure was used in the present study by employing the AM1 semi-quantitative method [16] to obtain the optimized geometry of **1**. The solid-state geometric parameters of **1** were used as input for the initial optimization of the fully relaxed molecule. The optimized geometry of **1** was used for the calculation of the moments of inertia ($I_{xx} = 376$, $I_{yy} = 449$, and $I_{zz} = 420$ amu Å$^2$), and the optimized C–H bond lengths were adopted for the relaxation calculations. The orientation of the inertial principle axis system with respect to the molecular geometry of **1** is shown in Fig. 1.

The final step of the numerical calculations utilized the powerful MOLDYN program [13b]. Among other functions, the program can be used to optimize parameter values for a given model expressed in the form of a spectral density function, and to provide the best fit to a set of experimental data. Any number of parameters may be optimized for a given model, provided that sufficient experimental data are available. Also, initial guesses and convergence criteria should be specified before proceeding with calculations. In addition, the program incorporates a subroutine for transformation of one Cartesian coordinate system to another. The optimization procedure is based on the SIMPLEX algorithm [13b] minimizing the normalized sum of squares of deviations between calculated and experimental relaxation data. This statistical parameter, the so-called target function, $F$ (Eq. 1), depends on the number of adjustable parameters, the precision and amount of experimental data, the ability of the model chosen to describe the range and types of motion present in the molecule, the convergency criteria, and the number of iterations for optimization.

$$F = \sum_{i=1}^{n} \left[ \frac{S_{i,\text{calc}} - S_{i,\text{exptl}}}{S_{i,\text{exptl}}} \right]^2 \tag{1}$$

where $S = T_1$ and/or NOE and $n$ represents the number of the experimental values.

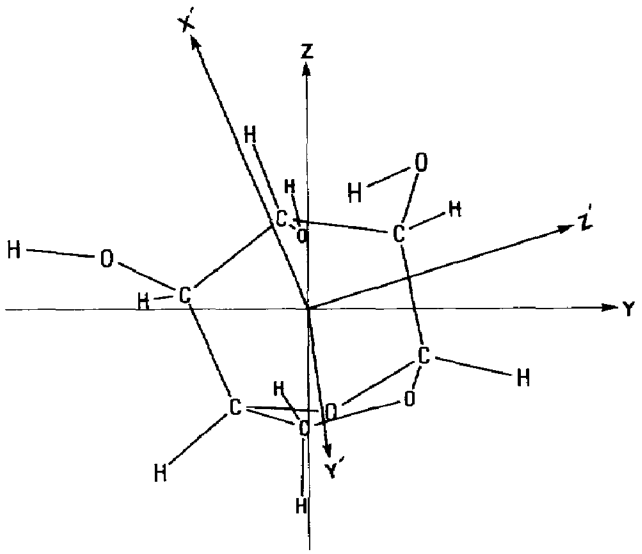

Fig. 1. Orientation of the principal axis system of the inertial tensor ($X'$, $Y'$, $Z'$) and that of the rotational diffusion tensor ($X$, $Y$, $Z$) for compound 1. The principal diffusion axis $X$ is perpendicular to the plane of the drawing.

The input parameters used by the program were the experimental $T_1$ values, geometrical data in terms of atomic coordinates, the number of direct and neighboring non-bonded $^{13}$C–$^{1}$H interactions, and the initial guesses for the three diffusion constants and the Euler angles $\alpha$, $\beta$, and $\gamma$. Since the Euler angles can be defined in several ways [16,17,19] it is important to give their definition for the present calculations. The transformation used in the MOLDYN program follows the definition of Whittaker [18]. The complete transformation is given by the three rotation matrices A, B, and C, i.e.,

$$T = CBA \tag{2a}$$

$$A = \begin{pmatrix} 1 & 0 & 0 \\ 0 & \cos\alpha & \sin\alpha \\ 0 & -\sin\alpha & \cos\alpha \end{pmatrix} \tag{2b}$$

$$B = \begin{pmatrix} \cos\beta & 0 & -\sin\beta \\ 0 & 1 & 0 \\ \sin\beta & 0 & \cos\beta \end{pmatrix} \tag{2c}$$

$$C = \begin{pmatrix} \cos\gamma & \sin\gamma & 0 \\ -\sin\gamma & \cos\gamma & 0 \\ 0 & 0 & 1 \end{pmatrix} \tag{2d}$$

These three successive rotations about the three Euler angles relate the principal axis system of the moment of inertia tensor, $I$, to the principal axis system of the rotational diffusion tensor, $D$.

$$D = TI \tag{3}$$

The optimization routine was executed initially for $\alpha = \beta = \gamma = 0°$ optimizing the diagonal elements of the rotational diffusion tensor. The obtained diagonal elements of the rotational diffusion tensor were then kept constant, while the Euler angles were optimized. Finally, the rotational diffusion constants as well as the angles were optimized simultaneously. Since the quality of the optimization depends on the initial guesses of the $D_i$'s, several starting values between $10^3$ and $10^{11}$ for the $D_i$'s were used, although MOLDYN is capable of giving the correct values even when the guess values are 50% of the true values. Independent of the starting values, either physically unreasonable values, or the same values for the optimized parameters always resulted. The guesses of $D_i$'s for the present calculations were $10^{10}$ $s^{-1}$.

The optimization procedure is based on the fact that the diagonal elements of the diffusion tensor. $D_{ii}$, are identical with the rotational diffusion constants, $D_i$ (diagonalization of the rotational diffusion tensor), only for the minima of the target function $F$, which is also a measure of the quality of the fit. Therefore, it is important to search for a minimum in $F$ by varying the Euler angles successively in small steps of 5°. Using this method of successive variations, it is possible to find all minima in $F$ by mapping of the $F$ values for different angle sets. In order to make sure that every minimum of $F$ was found, all gradients of $F$ were followed.

Following the above minimization approach many minima in the $F$ function were found, but only one was the global minimum. For instance, this minimum at 30 and 40°C was obtained for $\alpha = 50$, $\beta = 60$, and $\gamma = 40°$ with $F = 1.03 \times 10^{-3}$ and $2.9 \times 10^{-4}$, respectively. Numerical results for other arbitrary orientations of the rotational diffusion system gave values of $F$ larger by one to four orders of magnitude than for orientations for the global minimum in $F$. Some representative examples are as follows: $(\alpha, \beta, \gamma, F) = (0°, 0°, 0°, 2.32)$, $(-20°, 50°, 20°, 3.1 \times 10^{-1})$, $(50°, 60°, 30°, 5.8 \times 10^{-2})$, $(20°, -55°, 20°, 2.72 \times 10^{-3})$. Also, the values for the diagonal elements of the rotational diffusion tensor $D_{ii}$ differed by a considerable amount for these orientations, and even the order of their magnitude changed for some of them. The calculated diffusion constants are summarized in Table 2 for all temperatures.

## 3. Results and discussion

*Quantitative considerations of molecular motion.*—The general process in dynamic modelling of a monosaccharide in solution is to set up a TCF (dynamic model) that properly describes the various modes of reorientation in the molecule. The second step is to prove the ability of the model to describe the motion by reproducing the experimental relaxation data upon optimization of the adjustable parameters of the model (e.g., rotational diffusion constants, angular amplitudes, etc.). Finally, other dynamic models should be tested that may be capable of reproducing the experimental data as well. The last, and most important step, is to distinguish between models, since some of them may not correspond to the nature of the motion, and the fitting of the data may be no more than a computational exercise. The problem of discriminating between models can be solved, either by inspection of the geometry of the molecule, or by performing variable temperature relaxation measurements. The last approach is more rigorous and provides, in addition, activation energies which are useful kinetic parameters.

In the general case, the TCF for the overall motion is given by the following equation [20]:

$$G(t) = 5\sum_{a,a'}\langle D^{(2)*}_{qa}(\Omega_{LD}, 0)D^{(2)}_{qa'}(\Omega_{LD}, t)\rangle \tag{4}$$

The indices run from $-2$ to $+2$, and $D^{(2)}$ is the second order Wigner rotation matrix [21]. The angular brackets denote ensemble averages. The time dependent variable in Eq. 1 are the Euler angles $\Omega_{DL} = (\alpha_{LD}, \beta_{LD}, \gamma_{LD})$, which the molecular principal axes make with the laboratory axes. Within the framework of rotational diffusion, the average in Eq. 4 has been evaluated for isotropic [20], axially symmetric, and fully anisotropic motions [20,22,23].

Denoting the ensemble average in Eq. 4 by $\Gamma_{aa'}$, the following relationships hold:

Isotropic overall motion:

$$\Gamma_{aa'} = \delta_{aa'}(1/5)\ e^{-6D_o t} \tag{5}$$

Axially symmetric overall motion:

$$\Gamma_{aa'} = \delta_{aa'}(1/5)\ e^{-\lambda_a t} \tag{6}$$

Fully anisotropic overall motion:

$$\Gamma_{aa'} = (1/5)\sum_{r=-2}^{+2} Z(\lambda_r)_{aa'}\ e^{-\lambda_r t} \tag{7}$$

where $\delta_{aa'}$ is the Kronecker delta, $D_o$ is the isotropic diffusion constant, and the eigenvalues $\lambda_a = 6D_x - a^2(D_z - D_x)$ for the axially symmetric motion about the symmetry axis, $D_z = D\|$ and about the axis in the $(xy)$ plane perpendicular to the symmetry axis, $D_y = D_x = D_\perp$. Hubbard [22] has given expressions for the eigenvalues $\lambda_r$ and the eigenvectors $Z(\lambda_r)_{aa'}$ as a function of the rotational diffusion constants, $D_x$, $D_y$, $D_z$ of the overall motion about the $x$-, $y$-, and $z$-axis of the rotational diffusion tensor. Uusvuori and Lounasmaa [23] have tabulated these expressions in a more explicit form.

Fourier transform of the TCF's in Eqs. 4–7 provides the corresponding spectral density functions, $J(\omega)$, which for purely $^{13}C$–$^{1}H$ dipole–dipole interactions are related to the relaxation parameters $T_1$ and NOE by the following equations [1]:

$$\frac{1}{T_1} = (\Omega/20)\left[J(\omega_C - \omega_H) + 3J(\omega_C) + 6J(\omega_C + \omega_H)\right] \tag{8}$$

$$\mathrm{NOE} = \frac{\gamma_H}{\gamma_C}\,\frac{6J(\omega_C + \omega_H) - J(\omega_C - \omega_H)}{J(\omega_C - \omega_H) + 3J(\omega_C) + 6J(\omega_C + \omega_H)} \tag{9}$$

$$\Omega = N\left(\frac{\gamma_C\gamma_H\hbar}{r^3_{CH}}\right)^2$$

Here, $\omega_C$, $\omega_H$, $\gamma_C$, $\gamma_H$ are the Larmor frequencies and gyromagnetic ratios of the $^{13}$C and $^1$H nuclei, respectively, $\hbar = h/2\pi$ where $h$ = Planck's constant, $N$ is the number of the protons directly bonded to the carbon of interest, and $r_{CH}$ is the C–H internuclear distance.

Eqs. 6 and 7 describing anisotropic overall motion can be used under the assumption that the orientation of the principal axis system of the rotational diffusion tensor coincides with that of the moment of inertia tensor. Whether this assumption is valid or not depends on the symmetry of the molecule. The principal axes of the rotational diffusion tensor and those of the inertial tensor necessarily coincide only if a spherical-, linear-, or symmetric-top rotor, or an asymmetric-top rotor with at least two perpendicular mirror planes, is under consideration. For asymmetric-top rotors with lower symmetry the two principal axis systems need not necessarily be identical, provided that intermolecular interactions are strong enough [22,23].

The reason for the shift of the principal axes of both systems relative to each other is due to various intra- and/or inter-molecular factors. Thus, factors like the molecular shape, polar interactions, and/or hydrogen-bonding can cause the shift between both axis systems.

The molecular shape is strongly influenced by the presence of heavy atoms and can be responsible for the non-alignment of both principal axis systems [17,23]. Heavy atoms in small or medium sized molecules, such as bromine and iodine, do not affect the orientation of the rotational diffusion principal axes because of their mass, whereas they influence the inertial tensor and its principal axis system. Thus, for asymmetric rotors with less than two mutually perpendicular symmetry planes, the only reason for a displacement of the rotational diffusion principal axes from those of the inertial tensor in the presence of heavy atoms is the molecular shape. The shift between the two tensors is expected to be effective for asymmetric monosaccharides bearing a number of polar groups and hydrogen bonding centres.

There are several methods for determining the orientation of rotational diffusion tensor principal axes with respect to those of the inertial tensor depending on the molecular shape and the number of the non-equivalent C–H vectors in the molecule. For molecules with sufficient symmetry the orientation of the inertial principal axes can be determined by symmetry considerations. For asymmetric molecules, the inertial principal axis system must be found by diagonalization of the inertial tensor, $I$, which can be evaluated directly from the atomic masses and coordinates for an arbitrary coordinate system [13]. In order to transform the inertial tensor $I$ into its diagonal form, the eigenvalues $I_{ii}$ and the eigenvectors of the matrix $I$ must be evaluated. The eigenvalues give the moments of inertia. The eigenvectors form the transformation matrix, which yields by operation on the original coordinate system the principal axis system.

Such a diagonalization procedure cannot be used for the rotational diffusion tensor because not only the mass distribution in the molecule but also the intermolecular interactions in the liquid are required. Since intermolecular interactions are difficult to describe at a molecular level [17], it is not feasible, at present, to calculate the rotational diffusion tensor in an analogous manner to that

Table 1
$^{13}$C Spin-lattice relaxation times (s) [a] for **1** as a function of temperature at 50.3 MHz

| Temperature (°C) | C-1 | C-2 | C-3 | C-4 | C-5 | C-6 |
|---|---|---|---|---|---|---|
| 20 | 0.92 | 0.95 | 0.97 | 0.93 | 0.87 | 0.50 |
| 30 | 1.08 | 1.12 | 1.19 | 1.14 | 1.07 | 0.60 |
| 40 | 1.43 | 1.49 | 1.53 | 1.49 | 1.37 | 0.79 |
| 50 | 1.82 | 1.86 | 1.91 | 1.86 | 1.74 | 1.00 |
| 60 | 2.28 | 2.36 | 2.48 | 2.39 | 2.14 | 1.24 |
| 70 | 2.75 | 2.90 | 2.98 | 2.87 | 2.60 | 1.48 |
| 80 | 3.33 | 3.42 | 3.47 | 3.40 | 3.12 | 1.82 |
| 90 | 3.79 | 4.03 | 4.11 | 4.03 | 3.61 | 2.11 |

[a] Solutions, 0.5 M in dimethyl sulfoxide.

of the inertial tensor. Nevertheless, the rotational diffusion tensor (and the inertial tensor) is a symmetric tensor, and can always be transformed to its diagonal form. Since translation of the centre of diffusion does not affect the relaxation times, the rotational diffusion tensor is related to that of the inertial tensor by a rotation only [17,24]. In this respect, for the model of non-planar asymmetric-top molecule (Eq. 7), the three Euler angles relating the two principal axis systems should be determined together with the three rotational diffusion constants.

The Euler angles between both principal axis systems are calculated either as optimizable parameters simultaneously with the rotational diffusion constants in an optimization routine [17], or determined by means of successive variation of the angles [17,23]. In the first procedure, at least six linearly independent equations, and hence six unique C–H vectors, as well as their corresponding $^{13}$C $T_1$ values are needed for the determination of the six parameters, whereas for the second method the number of $T_1$ values may be less than six, but not less than three. Regardless of the method used, the success of the calculations is based on the fact that the best fit between experimental and calculated relaxation times is obtained only with the diagonal elements, $D_{ii}$, of the diagonalized rotational diffusion tensor. These values correspond to the rotational diffusion constants, $D_i$.

*Motional properties of 1,6-anhydro-β-D-glucopyranose* (**1**).— Table 1 collects the experimental $T_1$ values of all protonated ring carbons of **1** in dimethyl sulfoxide as a function of temperature. The NOE values of $2.988 \pm 0.05$ indicate that dipole–dipole interactions are the dominant relaxation mechanism, and that **1** tumbles in the region of fast motions Inspection of Table 1 reveals differences in the $T_1$ values of the ring carbons, which become more prominent at higher temperatures. The order is $2T_1$ (C-6) > $T_1$ (C-4) ~ $T_1$ (C-3) ~ $T_1$ (C-2) > $T_1$ (C-1) > $T_1$ (C-5). This trend in the $T_1$ values has been examined initially in terms of the C–H bond lengths and relaxation contributions from neighboring non-bonded protons. The C–H bond lengths obtained from geometry optimization of **1** were found to be: $r_{\text{C-1-H-1}} = 1.12$, $r_{\text{C-2-H-2}} = 1.12$, $r_{\text{C-3-H-3}} = 1.12$, $r_{\text{C-4-H-4}} = 1.12$, $r_{\text{C-5-H-5}} = 1.11$, $r_{\text{C-6-H-6}} = 1.11$, and $r_{\text{C-6-H-6'}} = 1.12$ Å. Assuming that these values represent a reasonable approximation of the true values, their relative magnitudes do not explain the differences in the $T_1$ data of their respective carbon atoms. Next the

Table 2
Rotational diffusion constants ($\times 10^{10}$ s$^{-1}$), target functions $F$ ($\times 10^{-3}$), activation energies (kJ mol$^{-1}$), $D_\infty$ values ($\times 10^{12}$ s$^{-1}$), correlation coefficients ($R$), and quotients [a] of the rotational diffusion constants for compound **1** (Euler angles, $\alpha = 50°$, $\beta = 60°$, $\gamma = 40°$)

| Temperature (°C) | $D_x$ | $D_y$ | $D_z$ | $F$ | $D_y/D_x$ | $D_z/D_x$ |
|---|---|---|---|---|---|---|
| 20 | 0.18 | 0.36 | 0.28 | 0.37 | 2.0 | 1.6 |
| 30 | 0.25 | 0.45 | 0.35 | 1.03 | 1.8 | 1.4 |
| 40 | 0.30 | 0.60 | 0.47 | 0.29 | 2.0 | 1.6 |
| 50 | 0.34 | 0.78 | 0.61 | 0.77 | 2.3 | 1.8 |
| 60 | 0.60 | 0.89 | 0.69 | 0.12 | 1.5 | 1.2 |
| 70 | 0.64 | 1.05 | 0.87 | 0.28 | 1.6 | 1.4 |
| 80 | 0.72 | 1.40 | 1.10 | 0.86 | 1.9 | 1.5 |
| 90 | 0.88 | 1.58 | 1.21 | 0.75 | 1.8 | 1.4 |
| $E_a$ | 20 | 19 | 19 | | | |
| $D_\infty$ | 6.4 | 7.2 | 5.9 | | | |
| $R$ | 0.98 | 0.99 | 0.99 | | | |

[a] $D_x/D_x = 1.0$ in all cases.

contribution of the intramolecular non-bonded C–H interactions to the relaxation of the various carbons of **1** was investigated by using the following equation for isotropic motion [1].

$$\frac{1}{T_1} = \sum_{i=1}^{n} \left( \frac{\gamma_H \gamma_C \hbar}{r_{CH,i}^3} \right)^2 \tau_c \qquad (10)$$

This equation assumes that $\tau_c$ is the correlation time for each $^{13}$C–$^1$H intramolecular interaction. The fit was poor over the whole temperature range studied. This molecule, therefore, must be approximated by an asymmetric-top rotor tumbling anisotropically in solution.

Table 2 contains the diagonal elements of the rotational diffusion tensor (i.e., the rotational diffusion constants $D_i$), and the target function $F$ for the minimum at all temperatures. The set of Eulerian angles which give the global minimum in $F$ was constant to within ±4% at all temperatures, indicating no significant shift of the rotational diffusion tensor principal axis system from the inertial tensor principal axis system by varying the temperature. For the set of Eulerian angles $\alpha = 50°$, $\beta = 60°$, $\gamma = 40°$ the order of the rotational diffusion constants is $D_y > D_z > D_x$. This trend is also reflected in the quotients of the rotational diffusion constants, $D_y/D_x$, and $D_z/D_x$ (Table 2), which describe the anisotropy of the rotational diffusion in solution. The principal axes of the rotational diffusion tensor corresponding to the aforementioned set of Euler angles is shown graphically in Fig. 1. In Table 3 the theoretical $T_1$ values obtained with the optimized parameters at the minimum are compared with the experimental $T_1$ data at 40 and 70°C. The relative deviation of the calculated $T_1$ values from the experimental ones is below ±3%, which is below the accuracy of the measurements. Similar good fits were obtained for the remaining temperatures (data not shown).

In order to illustrate the anisotropy of the rotational diffusion, and hence the influence of the intermolecular interactions, the square roots of the moments of

Table 3
Experimental ($T_{1,\text{exptl}}$) and calculated ($T_{1,\text{calcd}}$) $^{13}$C spin-lattice relaxation times [a] of **1** at 40 and 70°C

| Carbon atom | $T_{1,\text{exptl}}$ | | $T_{1,\text{calcd}}$ | |
|---|---|---|---|---|
| | 40°C | 70°C | 40°C | 70°C |
| C-1 | 1.43 | 2.75 | 1.43 | 2.76 |
| C-2 | 1.49 | 2.90 | 1.49 | 2.86 |
| C-3 | 1.53 | 2.98 | 1.55 | 2.98 |
| C-4 | 1.49 | 2.87 | 1.48 | 2.87 |
| C-5 | 1.37 | 2.60 | 1.36 | 2.62 |
| C-6 | 0.79 | 1.48 | 0.76 | 1.48 |

[a] In seconds.

inertia $(I_{yy}/I_{xx})^{-1/2} = 0.92$, $(I_{zz}/I_{xx})^{-1/2} = 0.95$, and $(I_{xx}/I_{xx})^{-1/2} = 1.00$ are compared with the quotients of the diffusion constants in Table 2. The values of the quotients of the diffusion constants show clearly that the rotational motion of **1** in solution is more anisotropic than when described by the rotational diffusion tensor for which the principal axes coincide with those of the inertial tensor. Thus, it appears that the diagonalized diffusion tensor should be used for the description of the rotational motion of **1** in solution.

It is interesting to note that the anisotropy in the diffusional reorientation of **1** is not affected by the temperature as can be seen from the nearly constant values of the quotients of the diffusion constants over the whole temperature range (Table 2). The values of $D_x$, $D_y$, and $D_z$ in Table 2 were plotted as a function of $1/T$ (K). From these linear, Arrhenius type plots (not shown) with correlation coefficients = 0.98–0.99, activation energies and values of $D_\infty$ for the free rotor were calculated and are summarized in Table 2. Although the activation energies may be in error by as much as 25%, their identical values indicate that the barrier heights for diffusion about the three principal axes of the diffusion tensor are not different from each other.

Huntress [24], and Gillen and Noggle [25] have described an approximate test to establish if reorientation of a molecule is diffusional or inertial about any particular axis. The $\chi_i$ value of the ratio between the diffusional and inertial motion is defined as [25]:

$$\chi_i = \frac{(\tau_o)_i}{(\tau_f)_i} = \left(\frac{5}{18}\right)\frac{1}{D_i}\left(\frac{kT}{I_{ii}}\right)^{1/2} \tag{11}$$

where $(\tau_f)_i$ is the mean time for a free rotor to rotate through 1 rad about the $i$th principal axis of the moment of inertia tensor, and $(\tau_o)_i$ is the molecular correlation time describing diffusion about the $i$th principal axis of the rotational diffusion tensor. A classification of the motion [25] can be carried out in terms of $\chi_i$ as follows:

| | |
|---|---|
| $\chi_i < 3$ | inertial region |
| $3 < \chi_i < 5$ | intermediate region |
| $\chi_i > 5$ | rotational diffusion region |

The calculated values of $\chi_i$ for the diffusion constants in Table 2 were found to be between 14 and 91, indicating that rotation about the $X$, $Y$, $Z$ principal axes of the diffusion tensor is diffusional in character over the entire temperature range studied. However, the results of the $\chi_i$ test must be considered with caution, since there is no coincidence between the inertial and rotational diffusion principal axes systems for the present molecule. In fact, in this case $(\tau_o)_i$ and $(\tau_f)_i$ values are the dynamic quantities referring to different orientations of the $i$th axis, so that only the ratio between the mean value $\langle\tau_o\rangle$ and $\langle\tau_f\rangle$ is representative for the dynamic region concerned. $\langle\tau_o\rangle$ and $\langle\tau_f\rangle$ are defined as:

$$\langle\tau_o\rangle = (6D)^{-1},\ D = (1/3)\ \mathrm{Tr}\{D\} \tag{12}$$

$$\langle\tau_f\rangle = \left(\frac{I}{kT}\right)^{1/2},\ I = (1/3)\ \mathrm{Tr}\{I\} \tag{13}$$

Another useful quantity that should be considered is the mean value of the angular velocity molecular correlation time $\langle\tau_J\rangle$, which is a measure of the efficiency of the molecular collisions, and describe the mean average time between internal collisions. This quantity is defined as:

$$\langle\tau_J\rangle = D\left(\frac{I}{kT}\right) \tag{14}$$

The calculated $\langle\tau_o\rangle$, $\langle\tau_f\rangle$, and $\langle\tau_J\rangle$ values for **1** are reported in Table 4. The $\langle\tau_o\rangle$ values are higher than the $\langle\tau_f\rangle$ values as a consequence of the strong intermolecular interactions in molecules **1**. This was expected since **1** has a large number of polar and hydrogen-bonding centres. The much smaller $\langle\tau_J\rangle$ with respect to the $\langle\tau_o\rangle$ and $\langle\tau_f\rangle$ indicate a large number of collisions per unit time. This fact supports the diffusion character of the rotational motion of **1** in dimethyl sulfoxide.

## Acknowledgment

Financial support from the University of Crete is greatly appreciated.

Table 4
Relative average values of the angular correlation times [a] in the vapor $\langle\tau_f\rangle$ and liquid $\langle\tau_o\rangle$ and the angular velocity correlation time $\langle\tau_J\rangle$ for **1**

| Temperature (°C) | $\langle\tau_f\rangle\times10^{-12}$ | $\langle\tau_o\rangle\times10^{-11}$ | $\langle\tau_J\rangle\times10^{-14}$ |
|---|---|---|---|
| 20 | 1.30 | 6.10 | 0.46 |
| 30 | 1.28 | 4.76 | 0.58 |
| 40 | 1.26 | 3.65 | 0.73 |
| 50 | 1.24 | 2.89 | 0.89 |
| 60 | 1.22 | 2.29 | 1.09 |
| 70 | 1.21 | 1.89 | 1.28 |
| 80 | 1.19 | 1.59 | 1.48 |
| 90 | 1.17 | 1.36 | 1.67 |

[a] In seconds.

## References

[1] J.R. Lyerla and G.C. Levy, *Top. Carbon-13 NMR Spectrosc.*, 1 (1974) 79–148.
[2] P.A.J. Gorin, *Adv. Carbohydr. Chem. Biochem.*, 38 (1981) 13–104.
[3] R.A. Komoroski, I.R. Peat, and G.C. Levy, *Top. Carbon-13 NMR Spectrosc.*, 2 (1976) 179–267.
[4] B. Coxon, *Dev. Food Carbohydr.*, 2 (1980) 351–390.
[5] P. Dais and G. Fainos, *Can J. Chem.*, 64 (1986) 560–565.
[6] P. Dais and A.S. Perlin, *Can J. Chem.*, 61 (1983) 1542–1548.
[7] P. Dais and A.S. Perlin, *Carbohydr. Res.*, 146 (1986) 177–191.
[8] P.J. Hajduck, D.A. Horita, and L.E. Lerner, *J. Am. Chem. Soc.*, 115 (1993) 9196–9201.
[9] A. Neszmélyi, A. Lipták, and P. Námási, *Carbohydr. Res.*, 58 (1977) c7–c9.
[10] M.F. Czarniecki and E.R. Thornton, *J. Am. Chem. Soc.*, 99 (1977) 8279–8282.
[11] P. Dais, T.K. Shing, and A.S. Perlin, *Carbohydr. Res.*, 122 (1983) 305–313.
[12] D.E. Axelson and C.E. Holloway, *Can J. Chem.*, 58 (1980) 1679–1686.
[13] There are several software packages used to calculate and transform the inertial tensor to its diagonal form. In this study two programs were used: (a) ATCOR2, Quantum Chemistry Exchange Program, QCPE 292, Indiana University, 1975; (b) D.J. Craik, A. Kumar, and G.C. Levy, *J. Chem. Inf. Comput. Chem.*, 23 (1983) 30–38.
[14] Y.-J. Park, H.S. Kim, and G.A. Jeffrey, *Acta Cryst. Sect. B*, 27 (1970) 220–227; K.B. Lindeberg, Acta Chem. Scand. *Ser. A*, 28 (1974) 1181–1182.
[15] L.D. Hall and L. Hough, *Proc. Chem. Soc.*, (1962) 382–367; D. Horton and J.D. Wander, *J. Org. Chem.*, 32 (1967) 3780–3788.
[16] M.J.S. Dewar, E.G. Zoebish, E.F. Healy, and J.J.P. Stewart, *J. Org. Chem.*, 107 (1985) 3902–3909; M.J.S. Dewar and K.M. Dieter, *ibid.*, 108 (1986) 8075–8086.
[17] A. Dolle and T. Bluhm, *Progr. NMR Spectrosc.*, 21 (1989) 175–201.
[18] E.T. Whittaker, *A Treatise on Analytical Dynamics of Articles and Rigid Bodies*, 4th ed., Dover Publications, New York, 1944, Chaps. 1–4.
[19] H. Goldstein, *Classical Mechanics*, Addison-Wesley, Reading, PA, USA, 1959, Chap. 4.
[20] D. Wallach, *J. Chem. Phys.*, 47 (1967) 5258–5268.
[21] M.E. Rose, *Elementary Theory of Angular Momentum*, Wiley, New York, 1957, Chap. 4.
[22] P.S. Hubbard, *J. Chem. Phys.*, 52 (1970) 563–568.
[23] R. Uusvuori and M. Lounasmaa, *Magn. Reson. Chem.*, 24 (1986) 1048–1068.
[24] W.T. Huntress, *J. Chem. Phys.*, 48 (1968) 3524–3533; W.T. Huntress, *Adv. Magn. Reson.*, 4 (1970) 1–37.
[25] K.T. Gillen and J.H. Noggle, *J. Chem. Phys.*, 53 (1970) 801–809.